Geosphere

Strike-slip faulting along the Wassuk Range of the northern Walker Lane, Nevada

Shaopeng Dong, Gulsen Ucarkus, Steven G. Wesnousky, Jillian Maloney, Graham Kent, Neal Driscoll and Robert Baskin

Geosphere published online 19 December 2013;
doi: 10.1130/GES00912.1

Notes

Geosphere, published online on 19 December 2013 as doi:10.1130/GES00912.1

Strike-slip faulting along the Wassuk Range of the northern Walker Lane, Nevada

Shaopeng Dong[1,2,*], Gulsen Ucarkus[3,*], Steven G. Wesnousky[2,*], Jillian Maloney[3,*], Graham Kent[4,*], Neal Driscoll[3,*], and Robert Baskin[5,*]

[1]*Key Laboratory of Active Tectonics and Volcanoes, Institute of Geology, China Earthquake Administration, Beijing 100029, China*
[2]*Center for Neotectonics Studies, University of Nevada Reno, Reno, Nevada 89557, USA*
[3]*Scripps Institution of Oceanography, University of California at San Diego, La Jolla, California 92093, USA*
[4]*Nevada Seismological Laboratory, University of Nevada Reno, Reno, Nevada 89557, USA*
[5]*U.S. Geological Survey, West Valley City, Utah 84119, USA*

ABSTRACT

A strike-slip fault is present outboard and subparallel to the Wassuk Range front within the central Walker Lane (Nevada, USA). Recessional shorelines of pluvial Lake Lahontan that reached its highstand ca. 15,475 ± 720 cal. yr B.P. are displaced ~14 m and yield a right-lateral slip-rate estimate approaching 1 mm/yr. The strike-slip fault trace projects southeastward toward the eastern margin of Walker Lake, which is ~15 km to the southeast. The trace is obscured in this region by recessional shorelines features that record the historical dessication of the lake caused by upstream water diversion and consumption. High-resolution seismic CHIRP (compressed high intensity radar pulse) profiles acquired in Walker Lake reveal ~20 k.y. of stratigraphy that is tilted westward ~20–30 m to the Wassuk Range front, consistent with ~1.0–1.5 mm/yr (20–30 m/20 k.y.) of vertical displacement on the main range-bounding normal fault. Direct evidence of the northwest-trending right-lateral strike-slip fault is not observed, although a set of folds and faults trending N35°E, conjugate to the trend of the strike-slip fault observed to the north, is superimposed on the west-dipping strata. The pattern and trend of folding and faulting beneath the lake are not simply explained; they may record development of Riedel shears in a zone of northwest-directed strike slip. Regardless of their genesis, the faults and folds appear to have been inactive during the past ~10.5 k.y. These observations begin to reconcile what was a mismatch between geodetically predicted deformation rates and geological fault slip rate studies along the Wassuk Range front, and provide another example of strain partitioning between predominantly normal and strike-slip faults that occurs in regions of oblique extension such as the Walker Lane.

INTRODUCTION

The Wassuk Range (Nevada, USA) is a north-trending ~80-km-long mountain block within the central Walker Lane (Figs. 1 and 2), which is an ~100-km-wide zone of discontinuous active faults and disrupted topography that trends along the east flank of the Sierra Nevada (e.g., Wesnousky, 2005). Based on geodesy, as much as one-fifth of the right-lateral relative plate motion between the Pacific and North America plates is accommodated east of the Sierra Nevada, with the majority localized within the Walker Lane (Bennett et al., 1999; Hammond and Thatcher, 2007; Thatcher et al., 1999). The eastern escarpment of the Wassuk Range is steep, abrupt, and bounded by a normal fault just west of Walker Lake (Fig. 2; e.g., Wesnousky, 2005). Here we present both terrestrial and lacustrine observations that place bounds on the late Pleistocene rate of uplift due to displacement on the range-bounding normal fault and document the presence of an active strike-slip fault system outboard and subparallel to the range front. The observations begin to reconcile

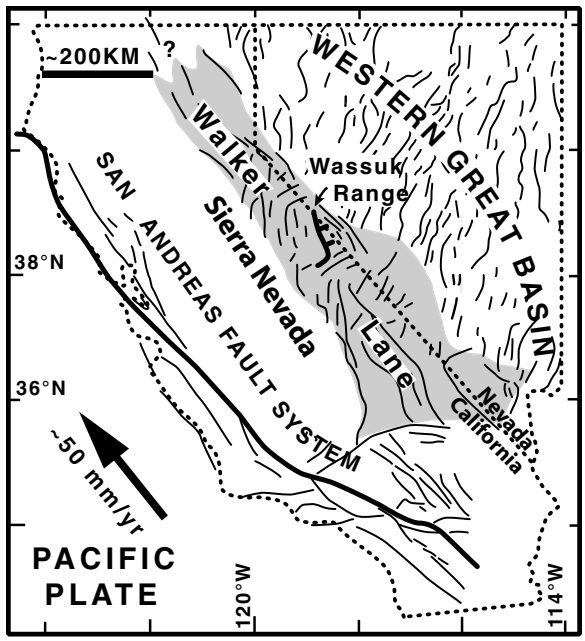

Figure 1. Tectonic map showing the location of the Wassuk Range within the Walker Lane (shaded). The range-bounding fault of the Wassuk Range is shown as a thick black line with hachures on the hanging wall. The majority of ~50 mm/yr of northwest-directed Pacific plate motion is taken up by the San Andreas and Walker Lane fault systems (adapted from Wesnousky, 2005).

*Emails: Shaopeng Dong: dshaopeng@gmail.com; Ucarkus: gucarkus@ucsd.edu; Wesnousky: wesnousky@unr.edu; Maloney: jmaloney@ucsd.edu; Kent: gkent@unr.edu; Driscoll: ndriscoll@ucsd.edu; Baskin: rbaskin@usgs.gov

Geosphere; February 2014; v. 10; no. 1; p. 40–48; doi:10.1130/GES00912.1; 8 figures.
Received 14 February 2013 ♦ Revision received 9 October 2013 ♦ Accepted 21 November 2013 ♦ Published online 19 December 2013

Geosphere, published online on 19 December 2013 as doi:10.1130/GES00912.1

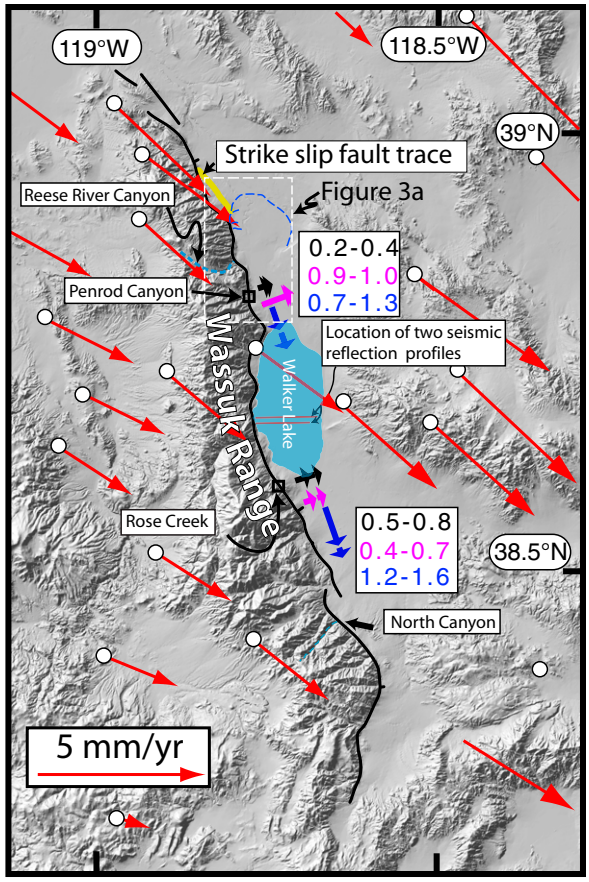

Figure 2. The range-bounding fault along the Wassuk Range is shown as a dark line. Global positioning system (GPS) measured displacement field (reported in Wesnousky et al., 2012) (red arrows emanating from small white circle) is plotted with respect to an assumed stable Sierra Nevada block. Orientation and increasing length of arrows to northeast show that shear is oriented oblique to the Wassuk Range. White boxes are geologically determined values of fault-normal extension (black—upper text), geodetic estimates of fault-normal extension (magenta—middle text), and geodetic estimates of fault-parallel strike slip (blue—lower text) (rates reported in Wesnousky et al., 2012). Two-headed arrows schematically show ranges of the same values and correspond in arrangement and color to the values in boxes. The geologically determined extension-rate arrows are placed adjacent to the sites of studies. The dashed white box shows the extent of Figure 3A. The dashed blue line approximates the 1252 m historical highstand shoreline of Walker Lake documented by Adams (2007) and marked in Figure 3A.

an existing mismatch between geodetically predicted deformation rates compared to geologically determined slip rates reported from studies along the range-bounding fault (Bormann et al., 2012; Wesnousky et al., 2012). The study also provides another example of the partitioning of slip between primarily normal and strike-slip faults that occur in regions of oblique extension (e.g., Wesnousky and Jones, 1994).

OBSERVATIONS

Terrestrial

The characteristics of the strike-slip fault system originally mapped by House and Adams (2010) are elucidated here with Lidar (light detection and ranging) data reported and processed by Lopes and Smith (2007) and a section of a 1:40,000-scale low-sun-angle photograph. The Lidar digital elevation map defines a lineament that is east of and strikes subparallel to the range front (Fig. 3). The entire lineament is located below the prehistoric highstand of pluvial Lake Lahontan that filled the basin to an elevation of ~1330 m ca. 13,070 ± 60 ^{14}C B.P. (e.g., Adams and Wesnousky, 1998), or ~15,475 ± 720 cal. yr B.P. (Briggs and Wesnousky, 2004). Below the ~1330 m pluvial highstand and above the ~1262 m latest Holocene highstand of the lake mapped by House and Adams (2009, 2010), the lineament cuts wave-washed surfaces of pluvial Lake Lahanton and alluvial fan deposits developed since that time. The field expression of the lineament is characterized by the presence of alternate facing scarps along strike, which are typically associated with strike-slip displacement (e.g., Wallace, 1991). The lineament continues southeastward from the ~1262 m shoreline for ~1 km as an alignment of vegetation. Continuing farther southeast with a slight change in azimuth, and below the ~1252 m A.D. 1868 historical highstand of the lake (Adams, 2007), a distinct lineament in the Lidar imagery is present (Fig. 3B). Though the Lidar reports horizontal and vertical positional accuracies of ~1 m and 13–20 cm, respectively, field observation indicates that the lineament is an artifact of Lidar processing errors (e.g., swath stitching misalignment).

An enlarged portion of a 1:40,000-scale Nevada Bureau of Mines and Geology low-sun-angle photo of the fault trace where it cuts recessional shorelines of Lake Lahontan is shown in Figure 4A. The fault trace cuts from northwest to southeast across the central portion of the image. Several of the tonal bands resulting from shadows cast by the recessional beach ridges are offset right laterally across the trace. To measure the amount of offset, the photo was georeferenced to existing U.S. Geological Survey digital raster graphics and orthophotoquads encompassing the site. The dashed line pairs in Figure 4B are along interpreted piercing point lines that follow the three most distinct tonal contrasts. The right-lateral offset of the tonal lineaments across the fault range from 11.7 to 15.2 m with an average of 13.5 m. In addition, we used a backpack global positioning system (GPS) to survey along our interpretation by eye of the crests and swales of a number of beach ridges (dotted line pairs in Fig. 4C). The range of 4 offsets measured in this way range from 12.3 m to 14.3 m, with an average of 13.9 m. Figure 4D shows the Lidar image at the same scale as Figures 4B and 4C. In this case, the offsets observed in the low-sun-angle image are not clearly evident in the Lidar image.

The offset shorelines postdate the highstand of pluvial Lake Lahontan (15,475 ± 720 yr B.P.). Dividing the ~14 m offset of the shorelines by the age of the highstand yields a minimum fault slip rate equal to ~0.9 mm/yr. The approximate fault slip rate assumes the total offset is due to multiple earthquakes.

Submarine CHIRP Survey

Methods

Approximately 200 line-km of seismic CHIRP (compressed high intensity radar pulse, acoustic variant) data were acquired in Walker Lake in 2012 and 2013 (Fig. 5). The survey employed Scripps Institution of Oceanography's Edgetech SUBSCAN CHIRP profiler and was operated with a 50 ms swept pulse of 1–15 kHz, which provides decimeter vertical resolution with subbottom penetration >60 m. All data were digitally recorded in JSF (Java Server Faces) format (converted to Society of Exploration Geophysicists SEG-Y format) with real-time GPS navigation, providing location accuracy to within 5 m. Data were processed using SIOSEIS (Scripps Institution of Oceanography seismic processing software; Henkart, 2005) and imported to IHS Kingdom Suite and IVS Fledermaus software packages for interpretation. A nominal water and sediment velocity of 1500 m/s is assumed for all depth and sediment thickness conversions.

Geosphere, published online on 19 December 2013 as doi:10.1130/GES00912.1

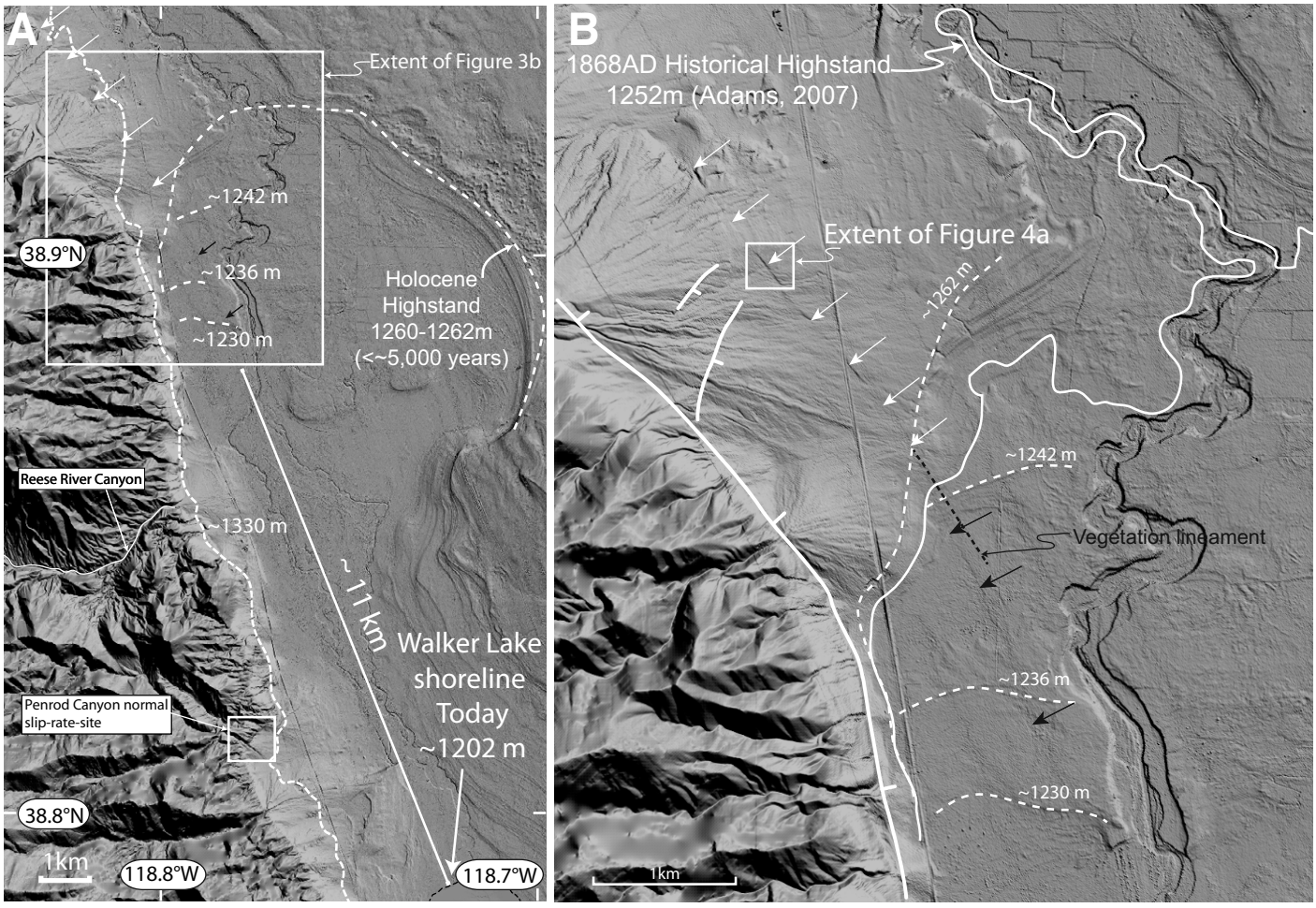

Figure 3. Portions of Lidar (light detection and ranging) imagery from Lopes and Smith (2007) along the west flank of the Wassuk Range with selected late Pleistocene and younger lake-level contours (dashed white lines) illustrated on the west side of the Walker Lake basin. The extent of this image is shown by the small box in Figure 2. (A) White arrows point to the location of fault trace outboard of the main range front. Walker Lake today is ~11 km south of the label of the 1230 m contour. (B) Enlargement of area in box in A. Fault trace (white arrows) extends southward below the historical 1868 A.D. highstand of Walker Lake as a lineament (black arrows) in the Lidar imagery. Although the Lidar data report horizontal and vertical positional accuracies of ~1 m and 13–20 cm, respectively, field observation indicates that the lineament is an artifact of Lidar processing errors. Small white box in B shows extent of aerial photo image shown in Figure 4.

Line D01L02 was designed to traverse across the locations of two existing cores acquired in the lake (12 and 50 m long; Benson, 1988; Bradbury et. al., 1989; Benson et al., 1991) to correlate the lithostratigraphy and seismic stratigraphy (Fig. 6). Detailed analyses of both cores were performed, including radiocarbon age dating (Benson, 1988; Bradbury et al., 1989; Benson et al., 1991), which allowed us to determine the age of the reflectors imaged in the CHIRP data as well as lake history (Fig. 6). These data provide important age constraints for the deformational events imaged in the CHIRP profiles. Accordingly, an unconformity associated with the horizon shown in orange in Figure 6 is interpreted to be ca. 20 ka and the age of the green horizon is interpreted as ca. 10.5 ka. In the shallow portion of the sedimentary section, an interpolation of ^{14}C-dated samples from the 12-m-long Benson et al. (1991) sediment core places the age of the blue horizon (erosional unconformity) as 3 ka and the age of the yellow horizon as ca. 3.9 ka. The distinct acoustic character of these reflectors allows for robust correlation of these horizons around the CHIRP seismic grid (e.g., Figs. 7 and 8).

Results

Characteristic track lines that best illustrate the structure and stratigraphy observed in the lake sediments are presented in Figure 6 (line D01L02), Figure 7 (line D01L01), and Figure 8 (line D02L13). All three lines cross the lake in the east-west direction (Fig. 5). There are several notable features observed in the CHIRP data. First and foremost, east-west profiles are marked by a strong divergence of sedimentary packages toward the Wassuk normal fault to the west. Superimposed on this westward tilt are broad folds, some faulted, with diminished amplitude upsection. The seismic imagery also reveals two erosional unconformities that appear to be related to periodic dessication of Walker Lake throughout the late Pleistocene and Holocene; these markers (orange, ca. 20 ka; blue, ca. 3 ka) also help place bounds on vertical slip rate across the Wassuk fault.

The divergence, rotation, and systematic increase in dip with depth of reflectors observed along the western portion of the lake (Figs. 6 and 7) are consistent with the presence of a

Geosphere, published online on 19 December 2013 as doi:10.1130/GES00912.1

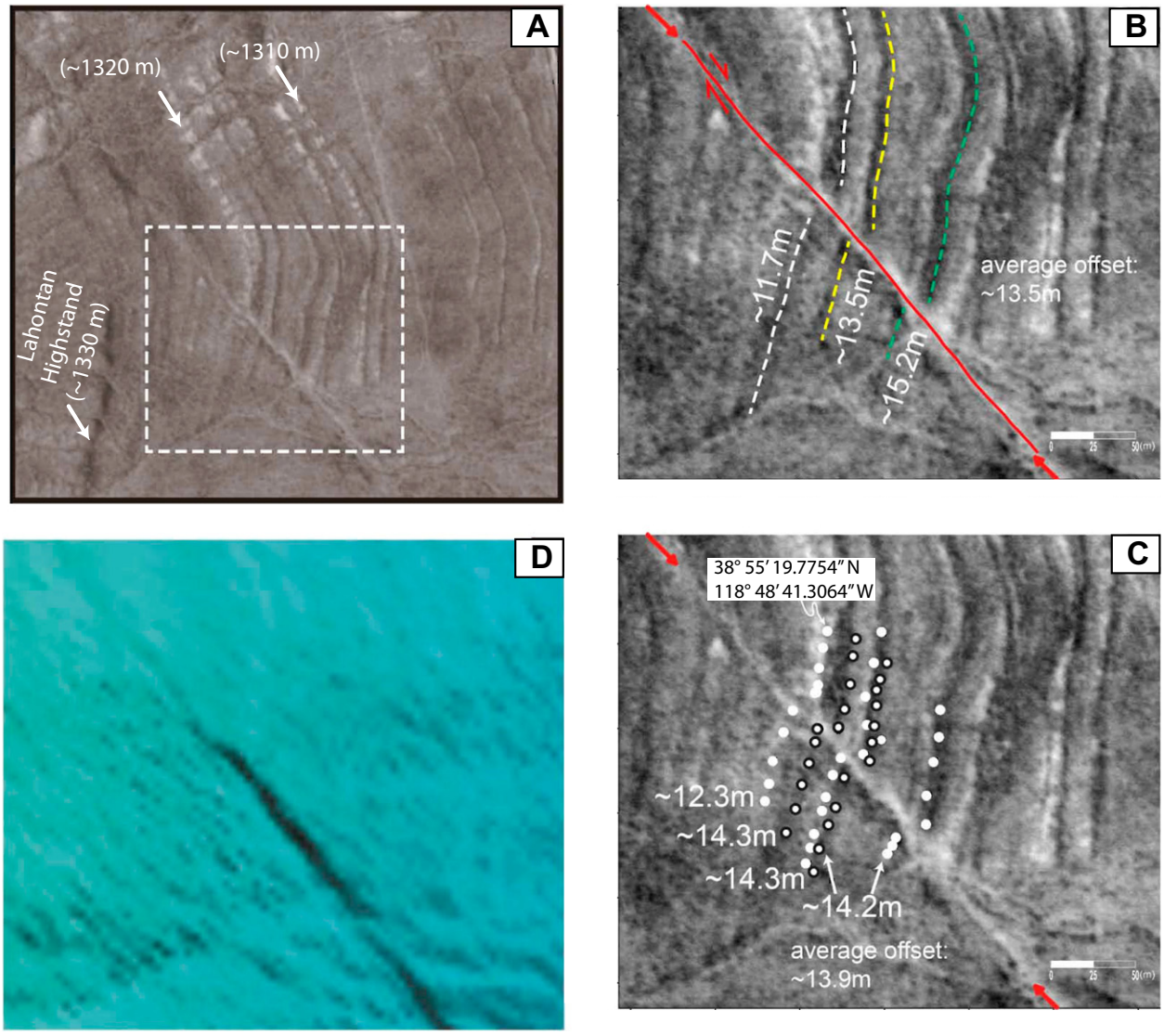

Figure 4. (A) Fault trace cuts from northwest to southeast across the enlarged portion of low-sun-angle photograph and shows right-lateral offset of tonal bands (shadows) that trend along the orientation of preserved recessional beach ridges of pluvial Lake Lahontan (Nevada Bureau and Mines and Geology Project Bell Photo NJ11–1, 1–836, 1:40K, 4–30–80). Location is shown by small box in Figure 3B. (B) Enlarged portion within dashed box of A shows different piercing lines defined by tonal contrasts (dashed lines) used to estimate fault offset. (C) White dots are backpack global positioning system (GPS) survey points along lines interpreted in the field to follow the crest and swales of the most evident recessional shoreline features. Latitude and longitude of a survey spot are annotated for further reference. The lineament between two red arrows shows the fault trace. Estimates of the offsets taken from these transects are annotated. (D) Lidar (light detection and ranging) image of same area as B and D extracted from data set of Lopes and Smith (2007).

down-to-the-east normal fault along the Wassuk Range front (e.g., Bormann et al., 2012). In this regard, the most recent deformation event preserved in the lake stratigraphy may be recorded by an ~2.5-m-thick sediment wedge above the blue horizon in Figure 6, which is dated as ca. 3 ka. Bormann et al. (2012) recognized at least one surface displacement during this period of time along the range-front fault at Rose Creek, and thus it is possible these events correlate. Alternately, the package of sediment above the sediment lense may reflect the infilling of a river channel that flowed across the dessicated lake surface that is represented by the blue horizon (erosional unconformity). The absence of reflectors and thus possible structures along the westernmost portion of the lake is attributed to the presence of gas in the sediments (Fig. 6).

The horizon depicted in orange (Fig. 6) exhibits a regional dip that increases toward the west near the core sites. The observed regional tilt to the west is ~20–30 m. Given that the horizon marks an erosional unconformity that was originally horizontal, the tilting would suggest a vertical component of displacement along the Wassuk Range front of 1.25 ± 0.25 mm/yr or more (20–30 m/20 k.y.). This value is more than twice that interpreted from displaced terrestrial deposits along the range-front fault (~0.2–0.8 mm/yr; Bormann et al., 2012; Fig. 2). The

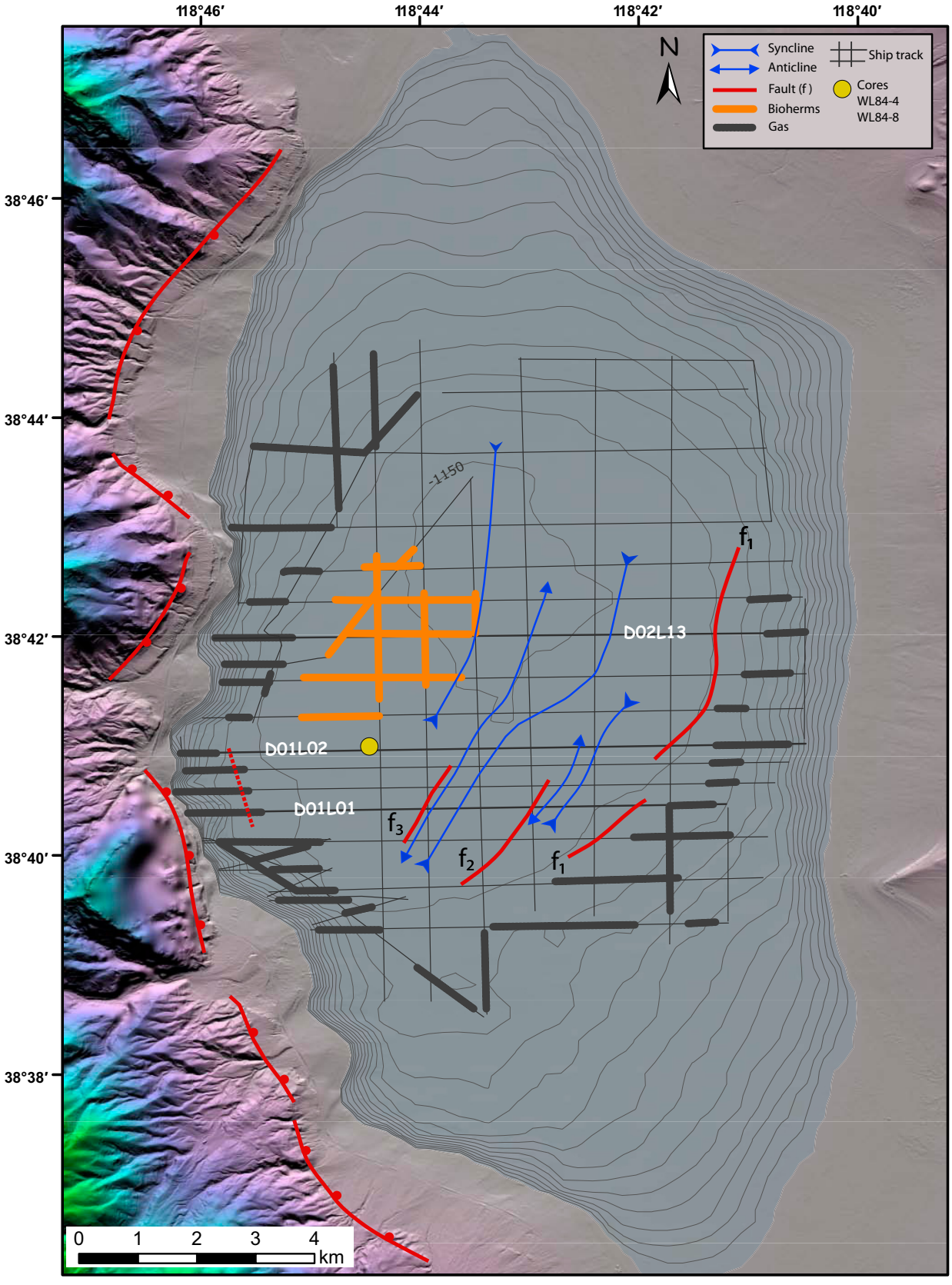

Figure 5. Topographic and bathymetric map of the Walker Lake region. Contour interval is 2 m. The legend highlights track lines from the CHIRP (compressed high intensity radar pulse) survey (black), core locations (yellow dot), Wassuk fault (red line with teeth), offshore antithetic faults (red lines within lake), fold axes (blue), and tufa and/or bioherm deposits (orange). D01L01, D01L02, and D02L13 are seismic profiles.

Geosphere, published online on 19 December 2013 as doi:10.1130/GES00912.1

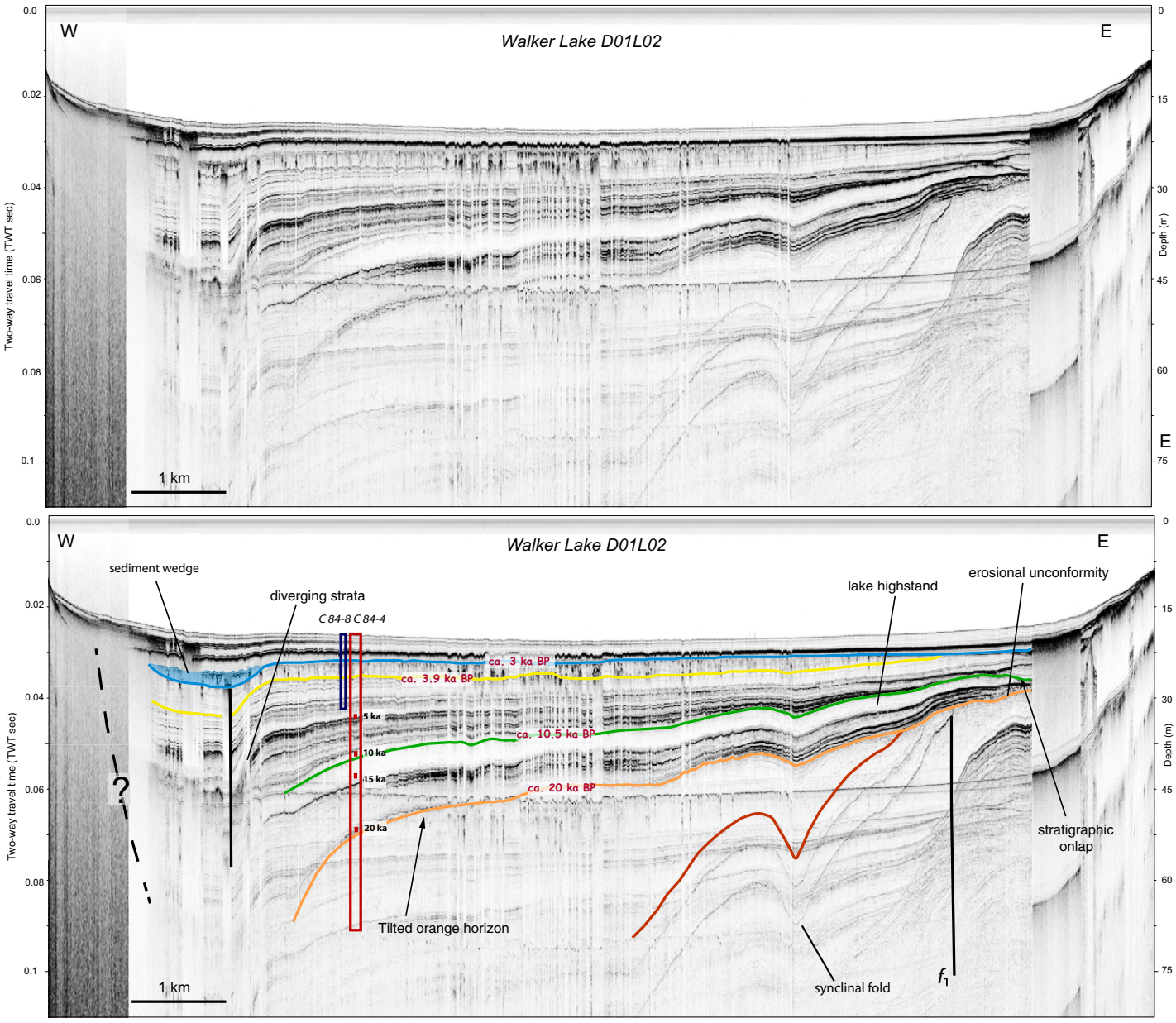

Figure 6. Uninterpreted (top) and interpreted CHIRP (compressed high intensity radar pulse) seismic profile D01L02 across Walker Lake. The ages of horizons are estimated by interpolating ^{14}C-dated samples from cores WL84-8 (Benson, 1988; Benson et al., 1991) and WL84-4 (Bradbury et al., 1989). Faults (*f*) are shown in black, sedimentary horizons are in various colors (see text for discussion). Key stratigraphic horizons are also annotated. The location of the CHIRP profile is shown in Figure 5. The vertical scale was converted from two-way traveltime (TWT) to meters using a nominal velocity of 1500 m/s. Horizontal scale bar is shown; vertical exaggeration is 65×. Dashed black line indicates a possible dip-slip fault.

difference in the estimated slip rate may reflect that the rates reported in each study are averaged over different periods of time or the limited data available to document the age of offset features in each study.

The deepest reflectors (horizons in red and below; Fig. 6) exhibit synclinal folds that diminish upsection: one in the case of line D01L02 (Fig. 6) and three in line D01L01 (Fig. 7). The layers of this deeper fold are concordant and maintain constant thickness. The easternmost limb of the easternmost fold in each section is truncated by an erosional unconformity (late Pleistocene, ca. 20 ka) marked for clarity in Figure 6 by an orange horizon that is most pronounced toward the east. This erosional unconformity is most likely due to wave-base erosion during an episode of lower lake level, possibly near Tioga glacial maximum of ca. 20 ka (Phillips et al., 1996).

The synclinal fold appears to continue upsection above the erosional unconformity, but with diminished amplitude. Clear evidence of tectonic folding is absent above the horizon in green; reflectors onlap within depressions on that horizon and appear to reflect the depositional infilling of the underlying fold (Fig. 6).

Geosphere, published online on 19 December 2013 as doi:10.1130/GES00912.1

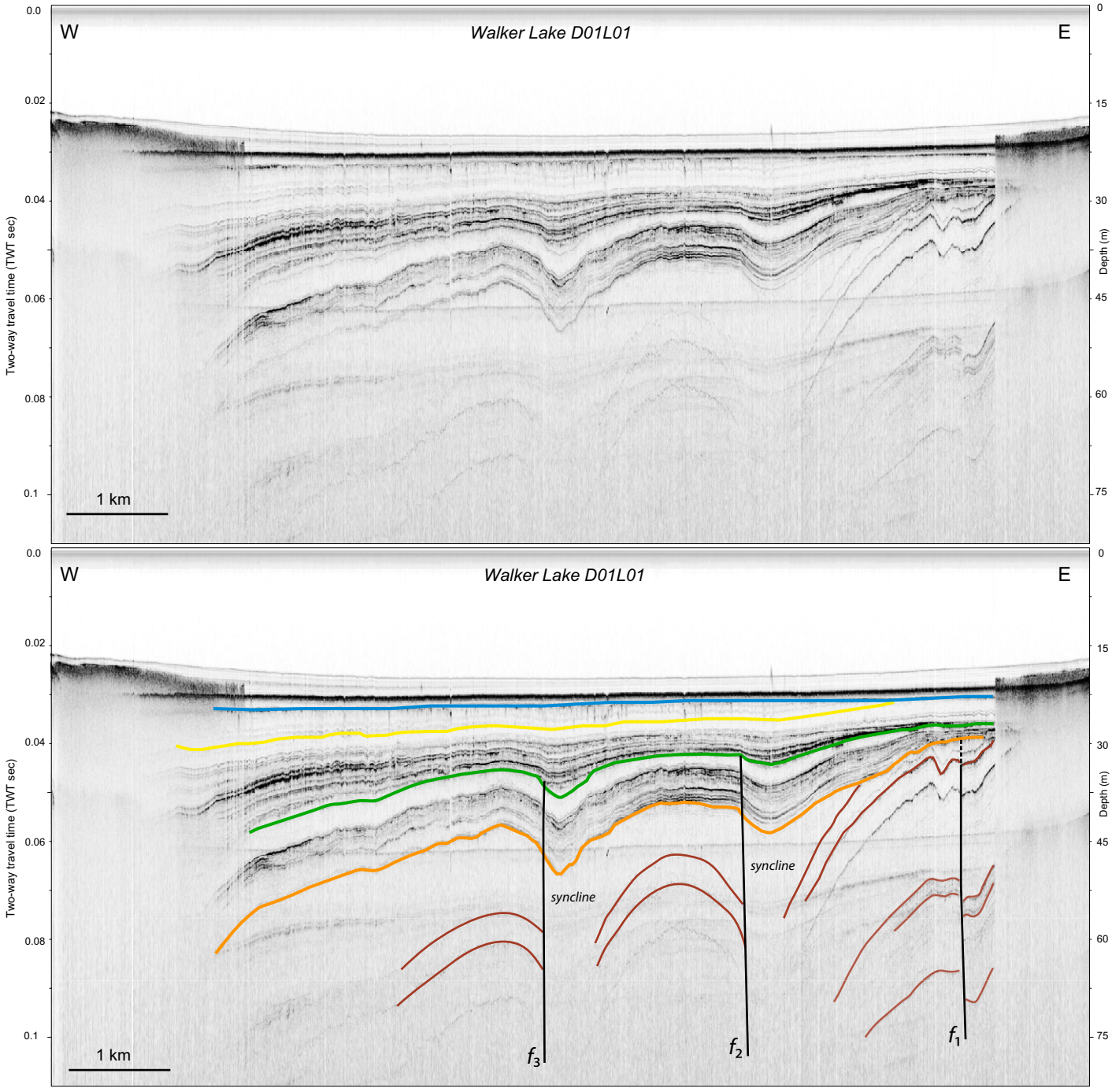

Figure 7. Uninterpreted (top) and interpreted CHIRP (compressed high intensity radar pulse) seismic profile D01L01 across Walker Lake. The location of the CHIRP profile is shown in Figure 5. Faults (*f*) are shown in black, sedimentary horizons are in various colors (see text for discussion). Horizontal scale bar is shown; vertical exaggeration is 65×.

The deepest basal reflectors are offset by a fault (f_1) along the easternmost fold on all three lines (Figs. 6–8). The different pattern of throw along this fault (f_1) (a different downthrown side is observed in D01L01 [Fig. 7] with respect to D02L13 [Fig. 8]) is consistent with strike-slip deformation. Deformation observed along this fault does not offset the orange horizon. In line D01L01 (Fig. 7), both of the two labeled synclines are offset at their western limbs with the cessation of deformation delineated by the green horizon (early Holocene, ca. 10.5 ka). Deduced age constraints for the orange and green horizons postdate the last deformational event associated with the deep folds and fold-related faults observed on all three lines ca. 20 ka (f_1) (Fig. 6) and 10.5 ka (f_2 and f_3) (Fig. 7).

The locations and orientations of fault and fold axes determined by mapping of these features through the entire CHIRP data set are summarized in Figure 5. The fault orientations and

Geosphere, published online on 19 December 2013 as doi:10.1130/GES00912.1

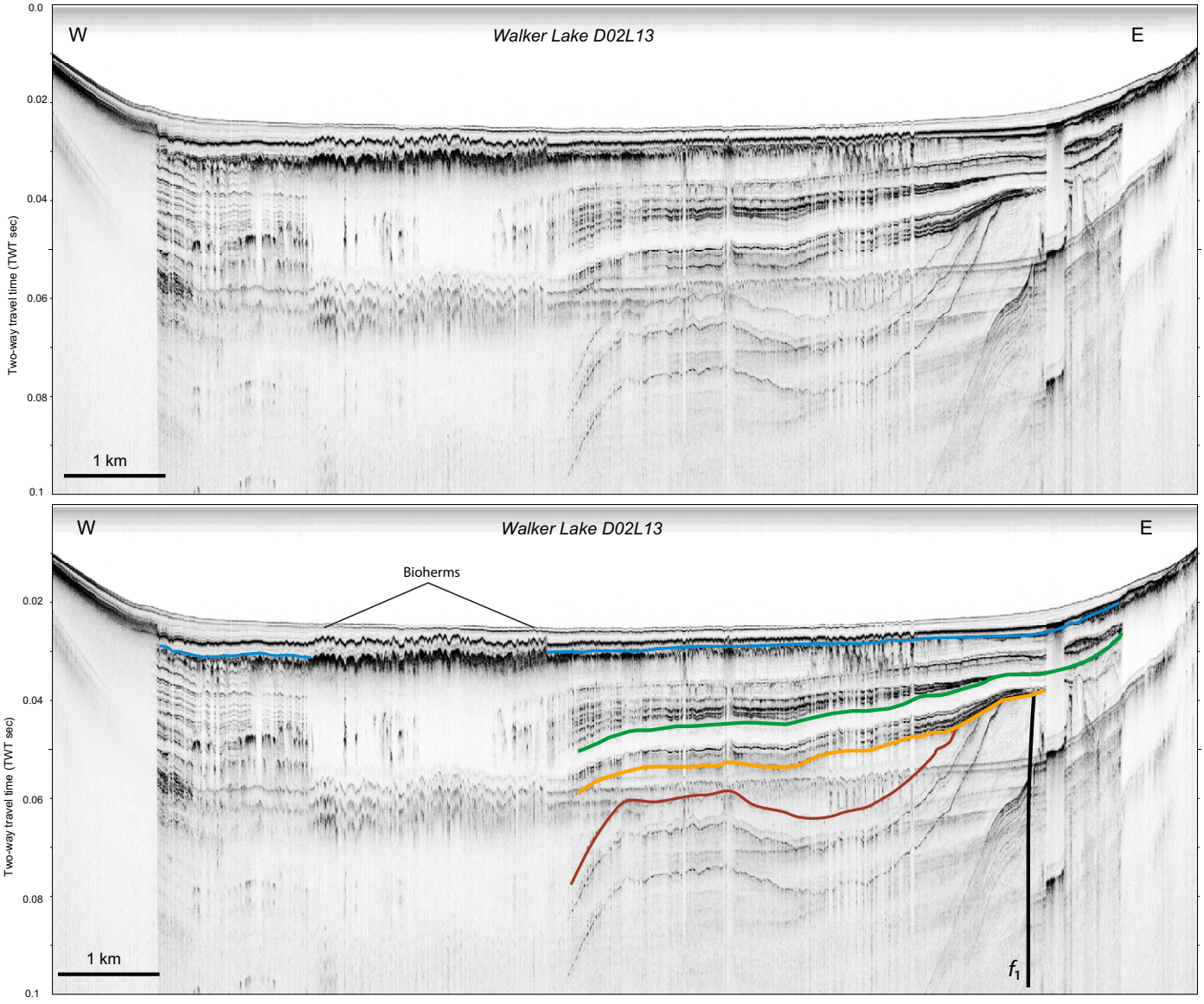

Figure 8. Uninterpreted (top) and interpreted CHIRP (compressed high intensity radar pulse) seismic profile D02L13 across Walker Lake. The location of the CHIRP profile is shown in Figure 5. Faults (*f*) are shown in black, sedimentary horizons are in various colors (see text for discussion). The locations of tufa and/or bioherms are highlighted (see text). Horizontal scale bar is shown; vertical exaggeration is 65×.

fold axes are oriented ~N35°E. The faults are discontinuous, are no more than 2–5 km long, and exhibit an en echelon character in map view (Fig. 5).

The CHIRP profiles also record lake-level fluctuations of Walker Lake in the late Quaternary that are consistent with several core studies (Benson, 1988; Benson et al., 1991). Benson (1988) reported high lake levels between 12 and 15 ka; this correlates to the acoustically transparent layer (homogeneous fine-grained sediments) below the horizon depicted in green (Figs. 6–8; ca. 10.5 ka). The green horizon is an onlap surface that separates the acoustically transparent highstand deposits below from the acoustically laminated onlapping sediments above. The high-amplitude reflectors within the acoustically laminated sequence are coarse layers emplaced during low-lake-level conditions (e.g., Brothers et al., 2011; Fig. 6). Some high-amplitude sequences are also observed above the orange layer, suggesting another lake-level lowstand that correlates with a desiccation period between 15 and 20 ka (Benson, 1988). Furthermore, the transparent layer below the orange horizon correlates to the highstand reported by Benson (1988) as older than 20 ka (Fig. 6). The acoustic character and erosional surfaces (i.e., orange and blue horizons, Figs. 6–8) observed in the CHIRP data appears in accord with the lake environment history as presented by Benson (1988) in terms of lake elevation and facies predictions from the late Pleistocene through Holocene.

A notable acoustic feature observed in the CHIRP data appears to be linked to distribution of tufas and/or bioherms in Walker Lake (Figs. 5 and 8). The pattern is well documented in line D02L13 (Fig. 8), where carbonate growth has resulted in a rough hummocky surface that obscures the sediments below. The attenuation of acoustic energy from the hummocky horizon is significantly different than acoustic attenuation by gas (Figs. 6–8). Acoustically, gas in the subsurface has a blotchy return and obscures reflec-

Geosphere, published online on 19 December 2013 as doi:10.1130/GES00912.1

tors beneath it. The hummocky surface has a marked change in roughness and a sharp acoustic impedance contrast. The distribution of the hummocky acoustic return is shown in Figure 5.

DISCUSSION AND CONCLUSION

Geodesy shows that at the latitude of the Wassuk Range, right-lateral strain accumulation across the width of the Walker Lane is equivalent to 6–7 mm/yr, with a lesser component distributed across the Wassuk Range front (Wesnousky et al., 2012). The Wassuk Range is oriented oblique to the shear field. As a result, it may be expected that both normal and strike-slip components of displacement are required to accommodate the ongoing shear. Prior geological estimates of fault slip rate are few, and focused on the component of normal displacement along the range-bounding fault (Bormann et al., 2012), suggesting that the vertical late Pleistocene slip rate along the range front is as much as ~0.7 mm/yr. Our observations of the divergence, rotation, and systematic increase in dip with depth of reflectors observed along the western portion of the lake allow that the vertical rate may be twice this value. An additional ~1.1 ± 0.4 mm/yr of right-lateral strike slip parallel to the range front is required by geodesy to account for the entirety of the geodetic strain field (Wesnousky et al., 2012). The terrestrial and lacustrine observations we have put forth here allow the suggestion that this additional ~1.1 ± 0.4 mm/yr may all, or in large part, be accounted for by slip on this strike-slip fault system outboard of the range front. The observed offset of the remnant Lake Lahontan shorelines is ~14 m. Dividing this value by the age of the Lake Lahontan highstand yields a slip rate of ~1 mm/yr; the rate assumes that the offset is the result of 2 or more earthquakes. Lesser offsets of these presumed events are not documented along the trace.

The partitioning of oblique deformation between subparallel normal and strike-slip faults was first noted by Fitch (1972) in his study of oblique convergence at plate boundaries; it has since been frequently observed in both transtensional and transpressional environments (Jones and Wesnousky, 1992; Wesnousky and Jones, 1994). In this particular case, it is analogous to the pairing of the Owens Valley and Sierran range-front faults farther south in the Walker Lane.

Projection of the strike-slip fault ~15 km southeastward toward Walker Lake is problematic. The trace is obscured over this distance by recessional shorelines features that record the historical dessication of the lake caused by upstream water diversion and consumption. Direct evidence for the existence of a northwest-directed right-lateral strike-slip fault is not present in the CHIRP profiles, although a set of folds and faults aligned along a N35°E trend, conjugate to the trend of the strike-slip fault observed to the north, is superimposed on the west-dipping strata. The presence of the faults and folds illustrates the presence of deformation within the lake. However, the explanation of the pattern and trend of folding and faulting beneath the lake is not simple, and may be due to development of Riedel shears in a zone of northwest-directed strike slip. While illustrative of late Pleistocene displacement, the faults and folds within the lake appear to have been inactive during the past ~10.5 k.y. If it is assumed that the onshore and submarine traces share the same earthquake history (i.e., that large earthquakes along the dextral strike-slip fault are driving deformation in the Riedel shear zone), it would imply that the ~14 m of offset observed onshore occurred during the same short period of time, perhaps due to a punctuated period of earthquakes lasting no more than ~5 k.y. The lack of a preserved strike-slip scarp below the 1260–1262 m middle to late Holocene shoreline (Fig. 3) supports the assumption underlying the idea.

ACKNOWLEDGMENTS

This is University of Nevada Center for Neotectonics Contribution 65. Funding for the seismic CHIRP (compressed high intensity radar pulse) survey on Walker Lake was provided by Southern California Earthquake Center award SCEC-10166. Support for Shaopeng Dong was provided by the China Earthquake Administration Grant No. IGCEA 1220 and the National Natural Science Foundation of China Grant No. 41372220. We thank Ken Adams for a constructive review and criticisms regarding the ages of the late Holocene and historical highstands of Walker Lake that were valuable in improving the paper. Constructive reviews by Angela Jayko and Cooper Brossy also improved the paper. We thank Danny Brothers for an internal U.S. Geological Survey review and Ernest Aaron for his equipment expertise.

REFERENCES CITED

Adams, K.D., 2007, Late Holocene sedimentary environments and lake-level fluctuations at Walker Lake, Nevada, USA: Geological Society of America Bulletin, v. 119, p. 126–139, doi:10.1130/B25847.1.

Adams, K.D., and Wesnousky, S.G., 1998, Shoreline processes and the age of the Lake Lahontan highstand in the Jessup embayment, Nevada: Geological Society of America Bulletin, v. 110, p. 1318–1332, doi:10.1130/0016-7606(1998)110<1318:SPATAO>2.3.CO;2.

Bennett, R.A., Davis, J.L., and Wernicke, B.P., 1999, Present-day pattern of Cordilleran deformation in the western United States: Geology, v. 27, p. 371–374, doi:10.1130/0091-7613(1999)027<0371:PDPOCD>2.3.CO;2.

Benson, L.V., 1988, Preliminary paleolimnological data for Walker Lake subbasin, California and Nevada: U.S. Geological Survey Water Resources Investigations Report 87-4258, p. 1–50.

Benson, L.V., Meyers, P.A., and Spencer, R.J., 1991, Change in the size of Walker Lake during the past 5000 years: Palaeogeography, Palaeoclimatology, Palaeoecology, v. 81, p. 189–214, doi:10.1016/0031-0182(91)90147-J.

Bormann, J.M., Surpless, B.E., Caffee, M.W., and Wesnousky, S.G., 2012, Holocene earthquakes and late Pleistocene slip-rate estimates on the Wassuk Range fault zone, Nevada: Seismological Society of America Bulletin, v. 102, p. 1884–1891, doi:10.1785/0120110287.

Bradbury, J.P., Forester, R.M., and Thompson, R.S., 1989, Late Quaternary paleolimnology of Walker Lake, Nevada: Journal of Paleolimnology, v. 1, p. 249–267.

Briggs, R.W., and Wesnousky, S.G., 2004, Late Pleistocene fault slip rate, earthquake recurrence, and recency of slip along the Pyramid Lake fault zone, northern Walker Lane, United States: Journal of Geophysical Research, v. 109, no. B8, doi:10.1029/2003JB002717.

Brothers, D., Kilb, D., Luttrell, K., Driscoll, N., and Kent, G., 2011, Loading of the San Andreas fault by flood-induced rupture of faults beneath the Salton Sea: Nature Geoscience, v. 4, p. 486–492, doi:10.1038/ngeo1184.

Fitch, T.J., 1972, Plate convergence, transcurrent faults, and internal deformation adjacent to southeast Asia and western Pacific: Journal of Geophysical Research, v. 77, p. 4432–4460, doi:10.1029/JB077i023p04432.

Hammond, W.C., and Thatcher, T., 2007, Crustal deformation across the Sierra Nevada, northern Walker Lane, Basin and Range transition, western United States, measured with GPS, 2000–2004: Journal of Geophysical Research, v. 112, no. B5, doi:10.1029/2006JB004625.

Henkart, P., 2005, SIOSEIS Scripps Institution of Oceanography seismic processing software package: http://sioseis.ucsd.edu.

House, P.K., and Adams, K.D., 2009, Preliminary geologic map of the southern part of the lower Walker River area, Mineral County, Nevada: Nevada Bureau of Mines and Geology Open File Map 09-13, scale 1:24,000.

House, P.K., and Adams, K.D., 2010, Preliminary geologic map of the northern part of the lower Walker River area, Mineral County, Nevada: Nevada Bureau of Mines and Geology Open File Map 10-12, scale 1:24,000.

Jones, C., and Wesnousky, S., 1992, Variations in strength and slip rate along the San Andreas fault system: Science, v. 256, p. 83–86, doi:10.1126/science.256.5053.83.

Lopes, T.J., and Smith, J.L., 2007, Bathymetry of Walker Lake, west-central Nevada: U.S. Geological Survey Scientific Investigations Report 2007-5012, 26 p.

Phillips, F.M., Zreda, M.G., Benson, L.V., Plummer, M.A., Elmore, D., and Sharma, P., 1996, Chronology for fluctuations in late Pleistocene Sierra Nevada glaciers and lakes: Science, v. 274, p. 749–751, doi:10.1126/science.274.5288.749.

Thatcher, W., Foulger, G.R., Julian, B.R., Svarc, J., Quilty, E., and Bawden, G.W., 1999, Present-day deformation across the Basin and Range province, western United States: Science, v. 283, p. 1714–1718, doi:10.1126/science.283.5408.1714.

Wallace, R.E., 1991, The San Andreas fault system: U.S. Geological Survey Professional Paper 1515, 283 p.

Wesnousky, S.G., 2005, Active faulting in the Walker Lane: Tectonics, v. 24, no. 3, doi:10.1029/2004TC001645.

Wesnousky, S.G., and Jones, C.H., 1994, Oblique slip, slip partitioning, spatial and temporal changes in the regional stress field, and the relative strength of active faults in the Basin and Range, western United States: Geology, v. 22, p. 1031–1034, doi:10.1130/0091-7613(1994)022<1031:OSSPSA>2.3.CO;2.

Wesnousky, S.G., Bormann, J.M., Kreemer, C., Hammond, W.C., and Brune, J.N., 2012, Neotectonics, geodesy, and seismic hazard in the Northern Walker Lane of western North America: Thirty kilometers of crustal shear and no strike-slip?: Earth and Planetary Science Letters, v. 329, p. 133–140, doi:10.1016/j.epsl.2012.02.018.